

Richard V. Snyder
 Frequency Engineering Laboratories
 Rt. 547 & Central Ave.
 Farmingdale, N.J. 07727

Abstract

Evanescence waveguide (rectangular or round) sections are used in conjunction with an admittance inverter synthesis technique incorporating frequency variable turns ratios to realize wideband microwave (up to 1 octave) and low frequency (60 MHz) low-loss bandpass filters. This work extends and corrects previous published information.

Introduction

In an informative paper, Craven & Mok [1] applied network synthesis techniques to lengths of below cutoff waveguide to obtain evanescent bandpass filters. It is the purpose of this paper to extend their work, introduce some slight corrections, and present various examples of the technique, including extension to low frequencies (down to 60 MHz) and to broadband filters (up to an octave). For wide stopband applications (no spurious recoveries until at least 1.5 fo) the structures will be shown to be more volumetrically efficient than others available.

Historical Difficulties

The work in [1], [8], and [9] has several limitations which must be overcome for general utilization of the technique. Filters designed using the methods contained in these references require that coupling reactances be invariant. This requirement limits the bandwidth over which an insertion loss function can be accurately predicted to 20% or less. Parasitic characteristics of the resonator capacitors were not included; thus bandwidth shrinkage and increased passband ripple resulted. Certain errors in the discontinuity susceptance formulae made difficult the realization of filters terminating in propagating waveguide. Data was not available on the Q of non-rectangular cross-sections. It was difficult to compute the length of the resonator capacitors. Finally, coupling methods presented were not suitable for broad bandwidths.

Design Technique & Results

The synthesis approach of [1] is illustrated in Fig. 3 of [1]. The admittance inverters utilize a simple equivalent circuit, a series inductor. Our approach is patterned after LEVY [2]. A more complete admittance inverter model is used in (Fig. 1) which incorporates transformers with frequency variable turns ratio. An equivalence similar to Fig. 8 of [2] is developed, with hyperbolic functions replacing circular functions. The use of a frequency variable turns ratio enables extension of the design technique of [1] to a full octave bandwidth. The mapping given by (19) of [2], in conjunction with eq. (2) of Fig. 3 relate the prototype transformer bandwidth to the filter length distribution resulting in a filter with the specified passband. Reference [1] has derived a correction factor between the frequency dependencies of the evanescent guide elements and those of the equivalent lumped elements. Applying this

factor Δ to eqn. (20) of [2], and then equating the resultant network to the lumped equivalent network, results in the design equations summarized in Fig. 3.

For filters with large bandwidths, it is necessary to work far enough below cutoff that eq. (2) of Fig. 3 has little variation due to change in Δ . For $f_c/f_o = 8$, an octave filter designed with a ripple of .01db achieved an actual ripple of approximately 0.1db (1.36 VSWR). The response is shown in Fig. 6. Fig. 2 illustrates the reactance vs. frequency characteristics of the equivalent elements comprising various lengths of below cutoff square waveguide. The dependencies far below cutoff are almost identically those of lumped inductors.

The actual design is accomplished through the use of an iterative computer program which apportions the inductive equivalent elements of the resonating capacitor to the series and shunt equivalent evanescent elements and thus "moves" the initially computed center spacing of the elements to compensate for their non-zero inductance. This inductance, uncompensated, effectively increased the series coupling reactance, thus decreasing the filter bandwidth. A procedure similar to that of Fig. 3 can be derived for filters starting with series resonators. The equivalent circuit is similar to Fig. 5 of [1], modified per eqn. (2) of our Fig. 3. Filters of this type, as in [1], are suitable for termination by above cutoff waveguide. Such a junction results in a combination E-plane, H-plane discontinuity. Using the method of LEWIN [3], equation (31) and (32) of [1] have been re-derived for rectangular cross-section.

$$3) \quad \eta_{HE} = \sqrt{\frac{ab}{Dd}} \quad \frac{1 - \left(\frac{D}{a}\right)^2}{\frac{a}{a_g} \cos \frac{\pi D}{2a}}$$

$$4) \quad B_{HE} = -\frac{1}{\omega \mu} \left\{ \frac{a_g}{a} \cot^2 \frac{\pi D}{2a} + \frac{a}{D} \eta_H^2 \right. \\ \left[\frac{b}{a_g} \left\{ \left(\frac{\pi}{D}\right)^2 - k^2 \right\} \ln \left(\csc \frac{\pi d}{2d} \right) - \frac{a_g}{a} \right. \\ \left. \left(\frac{b}{D} \right)^2 \left\{ \frac{1}{3} + \frac{1}{2} \left(\frac{d}{b} \right)^2 - \frac{8}{\pi^2} \frac{d}{b} \right\} \right] \right\}$$

WHERE $a_g = \sqrt{\frac{\lambda_0}{1 - \left(\frac{\lambda_0}{2a}\right)^2}}$, $\eta_H = \sqrt{\frac{a}{D}} \quad \frac{1 - \left(\frac{D}{a}\right)^2}{\frac{a}{a_g} \cos \frac{\pi D}{2a}}$

a = evanescent guide width
 b = evanescent guide height
 D = propagating guide width
 d = propagating guide height

η_{ME} = transformation ratio of admittance at the junction. The input sections of such filters are shortened to subtract the discontinuity susceptance computed in (4).

The design technique can be applied to non-rectangular cross-sections. In the appendix we derive the theoretical unloaded Q for a round cross-section utilizing an evanescent TE₁₁ mode. Plots of round section and square section Qu are shown in Fig. 4 (cutoff frequencies set equal). Computed filter lengths for identical bandwidths are also shown and are equal. Length is thus dependent solely on the cutoff frequency of the cross-section.

Fig. 3 enables computation of the tuning capacitance required for each resonator. It is necessary to subtract the fringing capacity associated with each resonator from the total. At lower frequencies the resonator may enter the wall of the filter. Fig. 5 illustrates the technique used to compute the total C_t .

To achieve large values of stopband in broadband filters, it is necessary to suppress the coupling between elements due to the degenerate TE₂₀ mode (rectangular cross-section). Small diameter inductive pins are installed (shown in Fig. 6) to perform this function. The effect of the pins is to cancel the coupling between the resonator posts due to the presence of higher order modes [4]. Using [4], the effect of the pins upon the resonator inductance can be calculated and included into the filter series coupling reactance as previously described. Various methods are available for coupling in and out of the filters. To compute the parameters of the coupling network (5) below, reproduced from [5], can be used.

$$(5) \quad Z_g = -\frac{B}{2A} + \sqrt{\frac{1}{4}(\frac{B}{A})^2 - \frac{C}{A}} \quad \text{WHERE } A = r_{22}, B = j(x_{\Delta} + x_{||}r_{22} - x_{22}r_{||}), C = x_{||}x_{\Delta} - r_{||}r_{\Delta}, \Delta = z_{11}z_{22} - z_{12}z_{21} - r_{\Delta} + jx_{\Delta}$$

This equation determines the impedance which will conjugately match the input and output of a linear two port, simultaneously. To use this equation, the impedance matrix of the synthesized filter is constructed, and the resultant elements used in (5). Typically, the coupling element must match into a very low impedance (7- ω or less) for shunt coupled filters, a' la' Fig. 3. Physically, the coupling takes the form of a small loop for bandwidths up to 15%, and a tap into the first resonator for wider bandwidths. Additionally, the coupling may consist of a two or three element lumped low pass filter with different input and output impedances. The filter response shown in Fig. 6 results from a cross-section measuring 0.5" x 0.5". No spurious passbands exist between 2 GHz and 15 GHz. Thus, the device stop bandwidth is comparable to that of a combine filter, with a $\lambda/18$ line length. The theoretical unloaded Q can be calculated using (50) of [1]. For the above examples (0.5" x 0.5", $f_0 = 1.5$ GHz), $Qu_{theo} = 3657$.

Through the use of the patented tuner assembly also shown in Fig. 6, we attain about 50% of the theoretical value while maintaining the ability to fine tune the center frequency of each element. While [1] referred to recovering 60% of the Qu on single sections, actual conversion of the multiple section filter response examples in [1] indicates about 30%. These filters have several mechanisms of spurious response:

1. When the resonator capacitors are spaced $\lambda_g/2$ above cutoff, a passband exists. This occurs from 10% to 100% above cutoff, depending upon filter bandwidth (resonator spacing).
2. At twice the TE₁₀ cutoff, the second mode (TE₂₀ in rectangular) will propagate. The resonators tend to act as short circuits to the TE₁₀, but due to location, will not reduce TE₂₀ significantly.
3. The coupling mechanism may resonate.

Filters have been built at 5 GHz with no spurious greater than 80db up to 40 GHz. These filters utilized WR-28 cross-section (21 GHz fc). These filters can be folded (with no degradation) for length compensation. Photographs of the inside of such filters will be shown (including a folded version of the aforementioned 5 GHz unit).

Applications

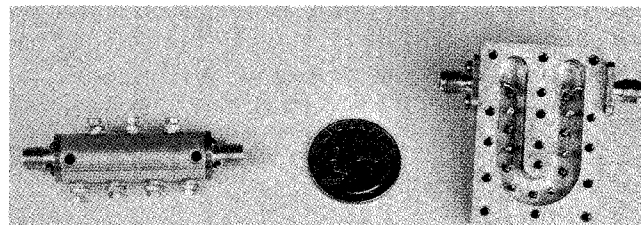
1. Bandpass filters with wide stopbands, and extreme package flexibility.
2. Clean-up filters in cascade with cavity filters, yielding low loss and wide stopbands.
3. I. F. filters. We have used lumped capacitors to realize filters with an unloaded Qu of 400 at 60 MHz in a cross-section of 1.5" x 1". The filters are loss-competitive with helical devices, but are much smaller.
4. In conjunction with item (3) above, the technique can be used to measure the Q of large value capacitors (the effective resonating inductance of the cross-section is very small). A later paper will present these rather disheartening results (most capacitors are very poor).
5. Component filters in multiplexers.

Conclusions

We have presented the elements of synthesis and some of the practical considerations necessary for the construction of evanescent filters with bandwidths up to an octave. The filters are lossier than propagating structures, but when it is necessary to cascade a second filter with a propagating filter for spurious suppression, it is often found that the resultant net insertion loss is greater than a single evanescent unit. The devices have great packaging flexibility, and have about 30% less volume than TEM designs with equivalent insertion loss. The structures are mechanical tolerance-insensitive, and are easy to fabricate. We expect to apply the evanescent high Q lumped tee or pi-equivalent circuit elements to many other networks including tunable filters and equalizers.

References

1. Craven & Mok, "Design of Evanescent Mode Waveguide Filters . . . Characteristic", Trans. MTT, March 1971.
2. R. Levy, "Theory of Direct-Coupled Cavity Filters", Trans. MTT, June 1967.
3. Lewin, L., "Advanced Theory of Waveguides", New York, Illife, 1951, pp. 88-100.
4. Lewin, L., "Theory of Waveguides", Halsted Press, 1975, sec. 5.13.
5. Snyder, R. & Bozarth, D., "Source & Load Impedance for Simultaneous Conjugate Match of Linear 2 Port", Electronic Communicator, Nov/Dec. 1967.
6. Craven & Lewin, "Design of Microwave Filters With Quarter Wave Couplings", Proc. IEE, Part B, 103, No. 8, pp. 173-177 (March 1956).
7. Ghose, R., "Microwave Circuit Theory & Analysis", McGraw-Hill 1963, pp. 168-171.
8. Mok, C. "Design of Evanescent-Mode Waveguide Diplexers", Trans. MTT, January 1973.
9. Edson, W., "Microwave Filters Using Ghost-Mode Resonance", Electronic Components Conference in San Francisco, May 2 - 4, 1961.
10. Nicholson, B.F., "Practical Design of Interdigital & Combline Filters", Radio & Electronic Engineer, July 1967, pp. 44-45.
11. Somlo, P., "Computation of Coaxial Line Step Capacitances", Trans. MTT, January 1967.



CIRCULAR TE₁₁ EVA-MODE

1 db PASSBAND
2200-2300 MHz

7 POLE

V.S.W.R. 1.25 MAX.
2200-2300 MHz

INSERTION LOSS
1.2 db AT 2250 MHz

FIRST SPURIOUS
ABOVE 20 GHz

FOLDED TE₁₀ EVA-MODE

1 db PASSBAND
5030-5090 MHz

7 POLE

V.S.W.R. 1.25 MAX.
5030-5090 MHz

INSERTION LOSS
2.5 db AT 5060 MHz

FIRST SPURIOUS RECOVERY
ABOVE 40 GHz

APPENDIX

Q_U FOR EVANESCENT TE₁₁ (ROUND CROSS SECTION) FILTER

WITH

$$(6) \quad \begin{aligned} H_2 &= J_1(k_c r) \cos \phi \\ H_\theta &= j \frac{1}{\eta} (1 - \frac{f_c^2}{f^2})^{1/2} \frac{f}{k_c r} \frac{f}{f_c} J_1(k_c r) \sin \phi \\ H_r &= -j \frac{1}{\eta} (1 - \frac{f_c^2}{f^2})^{1/2} \eta \frac{f}{f_c} J_1(k_c r) \cos \phi \\ E_r &= j \frac{\eta}{k_c r} \frac{f}{f_c} J_1(k_c r) \sin \phi \\ E_\theta &= j \eta \frac{f}{f_c} J_1(k_c r) \cos \phi \\ \eta &= \sqrt{\frac{4}{c}} \end{aligned}$$

MAXIMUM STORED ENERGY

$$(7) \quad W = \frac{4}{2} \iiint H \cdot H^* dV$$

AVERAGE DISSIPATED POWER

$$(8) \quad P = \frac{P_0}{2} \iint_{WALLS} H_{TRAN} \cdot H_{TRAN}^* dS$$

SUB (6) INTO (7)

$$W = \frac{\mu}{2} \int_V (H_2^2 + H_\theta^2 + H_r^2) dV$$

AFTER ALGEBRA

$$(9) \quad W = \frac{\mu}{2} \int_0^{\pi} e^{-2\pi z} dz \int_0^a J_1^2(k_c r) r dr \\ + \int_0^a \frac{1}{k_c^2} (1 - \frac{f_c^2}{f^2}) \frac{1}{r} J_1^2(k_c r) dr \\ + \int_0^a (1 - \frac{f_c^2}{f^2}) J_1^2(k_c r) r dr$$

SUB (6) INTO (8)

$$(10) \quad P = \frac{P_0}{2} \int_0^{\pi} \int_0^a / H_2 /^2 a d\phi dz \\ + \int_0^{2\pi} \int_0^a / H_\theta /^2 a d\phi dz$$

AFTER ALGEBRA

$$(11) \quad P = \frac{\pi a R_0}{2} \int_0^{\pi} e^{-2\pi z} dz J_1^2(k_c a) \left[1 + \frac{(1 - \frac{f_c^2}{f^2})}{k_c^2 a^2} \right]$$

DIVIDING (9) BY (11), AND LETTING $k_c r = v$

RESULT

$$(12) \quad Q_U = \frac{\omega M a}{R_0} \frac{A + (1 - \frac{f_c^2}{f^2})(\theta + c)}{J_1^2(k_c a) \left[-k_c^2 a^2 + (1 - \frac{f_c^2}{f^2}) \right]}$$

$$WHERE \quad A = \left(\frac{k_c a}{m} \right)^2 \sum_{n=1}^m \left(m - \frac{1}{2} \right) J_1^2 \left[\frac{k_c a}{m} \left(m - \frac{1}{2} \right) \right]$$

$$\approx \int_0^{k_c a} v J_1^2(v) dv$$

$$B = \sum_{n=1}^m \frac{J_1^2 \left[\frac{k_c a}{m} \left(m - \frac{1}{2} \right) \right]}{m - \frac{1}{2}} \approx \int_0^{k_c a} J_1^2(v) \frac{dv}{v}$$

$$C = -\frac{1}{4} \left(\frac{k_c a}{m} \right)^2 \sum_{n=1}^m \left(m - \frac{1}{2} \right) \left[J_0 \left(\frac{k_c a}{m} \left(m - \frac{1}{2} \right) \right) - J_2 \left(\frac{k_c a}{m} \left(m - \frac{1}{2} \right) \right) \right]^2 \\ \approx \int_0^{k_c a} v J_1^2(v) dv$$

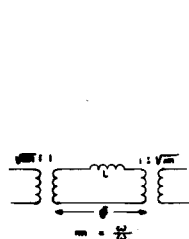
FOR TE₁₁ MODE, $k_c a = 1.64$ AFTER EVALUATION OF TERMS

$$(13) \quad Q_U = \frac{\pi \rho M d}{R_0} \left[\frac{.404 + .405 (1 - \frac{f_c^2}{f^2})}{1.144 + .338 (1 - \frac{f_c^2}{f^2})} \right]$$

WHERE

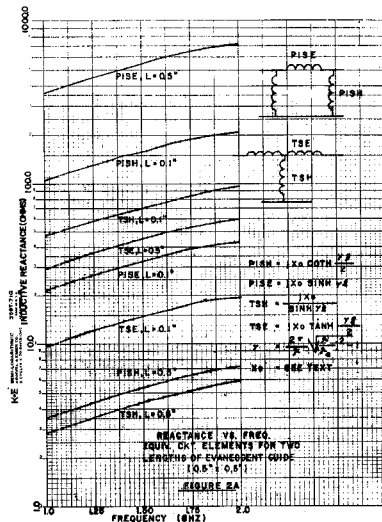
d = DIAMETER OF CROSS SECTION.

f_c = CUT-OFF FREQUENCY FOR CROSS SECTION.



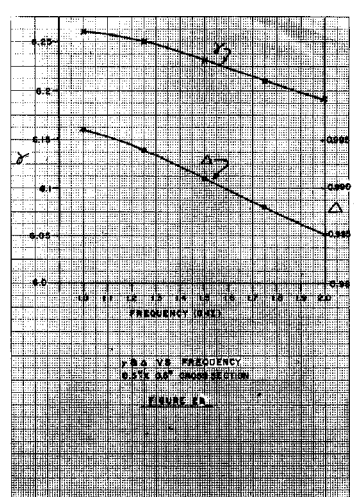
ADMITTANCE INVERTER
EQUIVALENT CIRCUIT

FIGURE 1



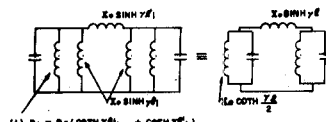
REACTANCE VS. FREQUENCY
FOR THE CIRCUIT ELEMENTS FOR TWO
LENGTHS OF EVANESCENT GUIDE
(0.5" & 0.1")

FIGURE 2A
FREQUENCY (GHz)



X vs. FREQUENCY
0.5" x 0.5" SQUARE SECTION

FIGURE 2B



(1) $B_1 = 8 \pi (COOTH YD)_{1-1} + COOTH YD^2$

WHERE $YD = \sqrt{V_{11,1-1}} = \sqrt{V_{11,1+1}}$

AND $YD = \frac{SINH YD}{2}$

$M = \frac{a}{2}$
FROM (3) $\Delta = \frac{a}{1 + (1/a)^2 YD^2}$

$Y = \frac{2\pi}{a} \sqrt{\frac{1}{a^2} YD^2 - 1}$

$X_0 = \text{CROSS-SECTION DEPENDENT}$

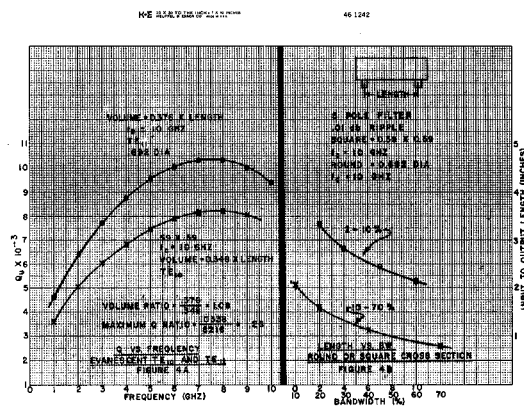
PROCEDURE
A) PROTOTYPE JUNCTION VSWR's V_1 SELECTED AS IN (2) WITH USE
OF (18), (17) & (18) OF (2).

NOTE THAT (2) OF (2) MAY BE USED TO APPROXIMATE (20) OF (2).
B) B_1 COMPUTED FROM (8) ABOVE.

C) CAPACITORS COMPUTED FROM (1) ABOVE.

DESIGN FORMULAE - SHUNT RESONATORS

FIGURE 3

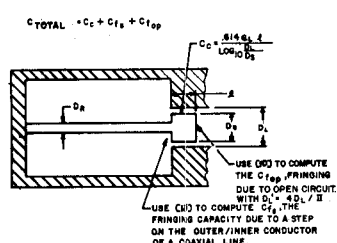


VOLUME RATIO VS. FREQUENCY

46-1242

HORN ON SQUARE CROSS SECTION

5

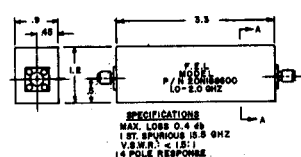


NOTES:

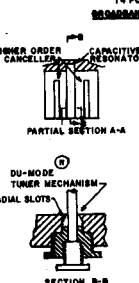
- 1) IF $D_2 \leq D_3$, C_1 MUST BE REDUCED AS IN (1) DUE
TO PROXIMITY EFFECT.
- 2) IF RESONATOR CAPACITANCE REQUIRED IS LOW, NO
WALL PENETRATION IS NECESSARY. ONLY C_{1op} IS
USED (PLUS C_{1s} TO END OF RESONATOR).

RESONATOR CAPACITANCE REALIZATION

FIGURE 5



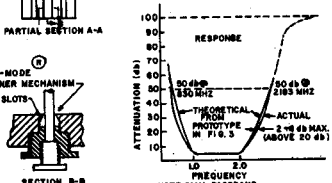
HIGHER ORDER MODE CANCELLER
CAPACITIVE RESONATOR



PARTIAL SECTION A-A
SECTION B-B
DU-MODE TUNER MECHANISM
4 RADIAL SLOTS

N = 14 FILTER CROSS SECTION 0.5" x 0.5" PASSBAND 1 - 2 GHz

FIGURE 6



ATTENUATION (dB)

FIGURE 6